Proceedings of the Annual General Donald R. Keith Memorial Conference
West Point, New York, USA
April 24, 2025
A Regional Conference of the Society for Industrial and Systems Engineering

GhostRoute: Energy-Aware, Detection-Minimizing Path Planning

Jacob Hyatt[1], James Grymes[1], Robert Jane[2], and Corey James[3]

[1]Department of Mathematical Sciences, United States Military Academy, West Point, New York 10996

[2]DEVCOM Army Research Laboratory, United States Military Academy, West Point, New York 10996

[3]Department of Chemistry and Life Science, United States Military Academy, West Point, New York 10996

Corresponding author's Email: thejacobhyatt@gmail.com

Author Note: CDT Jacob Hyatt is a cadet at the United States Military Academy majoring in Applied Statistics and Data Science. LTC James Grymes teaches in the Department of Mathematical Sciences at the United States Military Academy. Dr. Robert Jane is a Research Mechanical Engineer for DEVCOM Army Research Library. COL Corey James teaches in the Department of Chemistry and Life Sciences at the United States Military Academy. The views expressed herein are those of the authors and do not reflect the position of the United States Military Academy, the Department of the Army, or the Department of Defense.

Abstract: We present a methodology for autonomous vehicle route planning, balancing energy efficiency and stealth to enhance mission success. Our process transforms open-source satellite data into geospatial detection fields through evaluation of terrain, vegetation density, and enemy location. We then leverage network structures and integer programming techniques to minimize energy consumption and avoid detection. This approach enhances vehicle survivability and operational endurance, providing a critical advantage in contested environments.

Keywords: Unmanned Ground Vehicle, Satellite Imagery, Enemy Detection

1. Introduction

1.1. Background

Military autonomous vehicles, particularly electric or hybrid variants traversing terrain, are unlikely to complete their specific mission unless they can avoid detection and manage their onboard energy sources. These two critical criteria are often at odds with one another. Traditional path-planning algorithms historically optimize a single objective such as distance, energy consumption, or signature. This work employs a mixed integer non-linear programming approach to choose the best path for the vehicle while minimizing detection subject to the vehicle's power sources. Open source satellite data depicting terrain and foliage density is critical to the algorithm's ability to determine the best path with limited detection signatures. Additionally, we use enemy location intelligence to determine the line of sight risk and calculate real-time system exergy based on terrain features that the vehicle will traverse.

1.2. Literature Review

Path Finding Approaches. Path planning for unmanned ground vehicles (UGVs) has been extensively studied, with various approaches balancing computational efficiency, obstacle avoidance, and stealth considerations. In a static 2D environment, both A* and the H2A heuristic algorithm have been used to navigate UGVs while avoiding obstacles (Almoaili & Kurdi, 2020). The H2A algorithm prioritizes paths that maximize the distance from obstacles while maintaining computational efficiency, performing faster than A*. However, these methods do not account for complex mission constraints such as energy expenditure and enemy detection constraints. Our model takes into account the location of multiple enemy and the threat that they might pose to the UGV, while also balancing the energy constraints of the UGV. Many researchers have contributed to the advancement in path planning for UGVs such as the Minimal Exposure Dubins Orienteering Problem (MEDOP) which is a novel multi-objective formulation tailored for autonomous vehicles operating in environments with predefined sensor fields. The primary objectives are twofold: maximizing the collection of rewards from target locations and minimizing the vehicle's exposure to detection (Macharet, Neto, & Shishika, 2021). This work, however, does not consider energy expenditure. Likewise, others have sought to find energy-optimal paths such as littoral path planning work for unmanned surface vehicles (USVs), aiming to find paths that are not only short and smooth but also energy-efficient and safe (Ma, Hu, & Yan, 2018). We seek to extend this work by incorporating detection considerations.

Battery Discharge Modeling. Accurately modeling battery behavior is essential for optimizing UGV energy endurance. Prior work has demonstrated the nonlinear discharge characteristics of Nickel-Metal Hydride (NiMH) batteries, highlighting how power depletion follows a nonlinear curve based on load conditions (Jane et al., 2017). Effective power management strategies ensure mission completion by preventing unexpected energy depletion. Our approach builds on these principles by incorporating power management, ensuring that the UGV dynamically adjusts its path and charging behavior to extend mission duration.

Sound Profiles. The acoustic signature of a UGV plays a significant role in stealth operations. Research has shown that electric vehicles (EVs) and internal combustion engine (ICE) vehicles exhibit significantly different sound profiles, particularly at low speeds (Juhari, Salleh, Muhamad, & Ito, 2013). While EVs are notably quieter in low-speed maneuvers, their sound levels converge with ICE vehicles at higher speeds (Juhari et al., 2013). We utilize this work when determining our dB levels for our audio detection functions. We treat the UGV as an EV when the generator is off, and when it is on we treat the UGV as a ICE vehicle.

Probabilistic Detection Models. Avoiding detection is a fundamental challenge in autonomous vehicle operations, particularly in adversarial environments. Probabilistic threat modeling has been effectively applied to unmanned aerial vehicles (UAVs) to compute paths that maximize the likelihood of escaping detection (Pfeiffer, Batta, Klamroth, & Nagi, 2007). We extend these probabilistic techniques to ground-based UGV operations, integrating energy-aware path planning with detection avoidance to enhance survivability in contested areas.

2. Methodology

Our work introduces a three-phase methodology. The first phase collects the operational intelligence, such as terrain analysis and enemy location; phase 2 transforms the operational intelligence into a node network that includes a detection field and energy use; and the third phase utilizes the node network to create an optimal tactical route for mission execution. Our system is initialized with satellite imagery and elevation data from our area of interest. We create a two-layered grid, one layer for standard vehicle operations and another for operating the generator to charge the onboard battery energy storage system, and lay it over the images to act as nodes. The operation of the generator increases the noise and therefore increases the likelihood of detection. This grid creates a discretized area of operations for our optimization algorithm. An example of this grid can be seen in 1b. The images are used as inputs to compute arc costs for both detection and energy. The costs are fed into our mixed integer non-linear program, modeled in Julia's modeling language JuMP, and solved with the Gurobi optimization software that produces routes that minimize detection while considering energy. An overview of our approach is seen in Figure 1a.

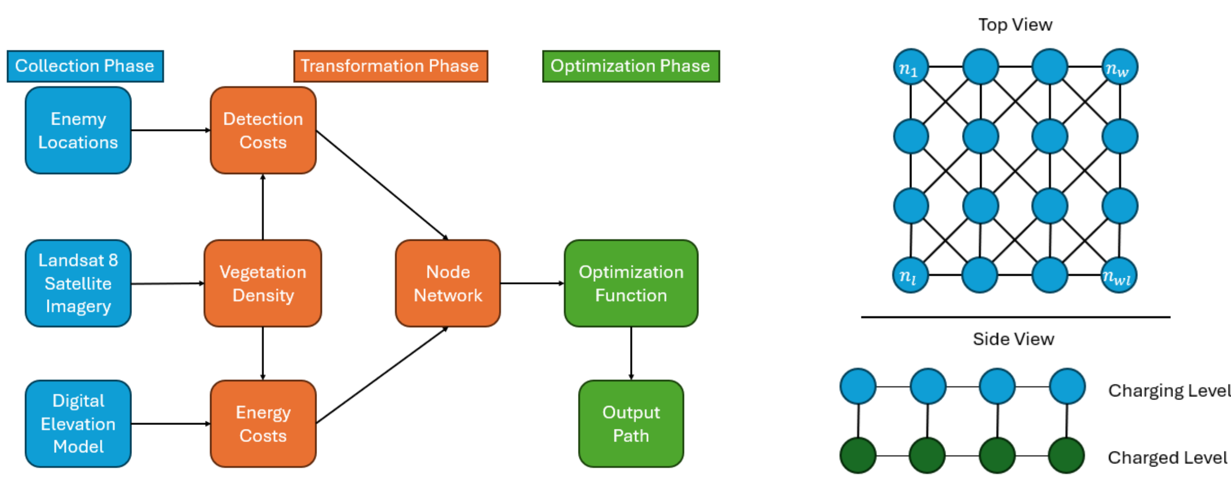

(a) Flow diagram depicting the process of data and intelligence collection, transformation to modeling data, and solving the optimization model.

(b) Node network example for a 4 by 4 grid of nodes.

Figure 1: Overview of the modeling process and an example network representation.

ISBN: 97819384969-9-8

2.1. Building the Operational Terrain Intelligence Layer

2.1.1. Remote Sensing for Terrain Analysis

Satellite imagery in this study was obtained from the United States Geological Survey (USGS). We download both Landsat 8 images and the corresponding digital elevation model (DEM) for the area of interest. The Landsat 8 data includes multiple spectral bands, covering portions of the visible, near-infrared (NIR), and shortwave infrared (SWIR) spectrum. The DEM, on the other hand, is a grayscale representation of the Earth's topographic surface, capturing elevation changes while excluding surface objects such as trees and buildings. To ensure accurate spatial representation, we preprocess the data in ArcGIS by aligning the geospatial coordinates. To quantify vegetation density, we compute the Normalized Difference Vegetation Index (NDVI), a widely used metric derived from Landsat 8 imagery (Rouse, Haas, Schell, & Deering, 1974).

$$\mathrm{NDVI} = \frac{\mathrm{NIR} - \mathrm{Red}}{\mathrm{NIR} + \mathrm{Red}} \tag{1}$$

NDVI utilizes the differences in how vegetation reflects and absorbs light at different wavelengths (Huang, Tang, Hupy, Wang, & Shao, 2021). Equation (1) shows the calculation of NDVI. The red band corresponds to visible light, which is absorbed by the green in plants. In contrast, the NIR band represents wavelengths that vegetation reflects efficiently due to plant leaves. As a result, healthy, dense vegetation has high NDVI values, while barren land and non-vegetated surfaces exhibit lower values. The index ranges from -1 to 1, where negative values typically indicate water, values near zero correspond to bare soil, rocks,or urban areas, and values closer to 1 signify dense, healthy vegetation.

2.1.2. Utilization of Digital Elevation Model

To extract elevation from the digital elevation model (DEM), we utilize the pixel intensity values in the grayscale DEM imagery. Since DEM data represents elevation in a raster format, each pixel's brightness corresponds to a specific elevation value, with darker pixels indicating lower elevations and brighter pixels indicating higher elevations. The elevation at a given node is calculated using Equation (2):

$$E(x, y) = \frac{N_k^{(\mathrm{x,y})}}{255} E^{\mathrm{max}} \tag{2}$$

Here, $N_k^{(\mathrm{x,y})}$ represents the pixel intensity value at node k, while 255 is the maximum possible intensity value for an 8-bit pixel. E^{max} denotes the maximum elevation in the area of operations. This normalization ensures that pixel intensities are proportionally scaled to actual elevation values, enabling accurate interpretation of terrain variations. Utilizing the 2 allows for a seamless integration into the creation of node weights. By integrating elevation data from the DEM with spectral information from Landsat 8 imagery, we enhance our spatial analysis by accounting for both vegetation cover and topographic influences.

2.2. Detection Field Generation

To calculate detection weights, we utilize both audio and visual detection functions. The audio function accounts for the decibel level generated by the unmanned ground vehicle (UGV) as it travels, applying a sound attenuation function to simulate the propagation of sound to an enemy observer. The visual function applies a probability of detection by calculating the total area that the UGV takes up in the seeker's field of view (Blackmon, 2022). For each arc, both audio and visual detection probabilities are computed, and we assign the maximum of these values as the detection value for that arc. While this method ensures a conservative estimate of detection, alternative aggregation methods could also be explored. These aggregation methods could be a simple average between audio and visual functions or a proximity-based approach, switching to one method as the UGV gets closer to the seeker.

2.2.1. Audio Detection

The noise levels generated by the UGV vary throughout the region based on vegetation density along the arc and whether the generator is actively charging the onboard battery. We use vegetation density values derived from the NDVI to determine the UGV's point source noise level. This point source represents the decibel level produced by the UGV after accounting for environmental factors. The UGV has a baseline noise level of 40 dB when moving on an improved surface. In dense vegetation, its noise level rises to 75 dB due to moving through a non-improved surface, such as a wooded area. When charging, the UGV also produces 75 dB of noise, regardless of vegetation density, since the generator overpowers the sound of movement. These dB levels are assumed based on dB readings from electric vehicles and comparably sized generators as we

ISBN: 97819384969-9-8

are unable to get readings from the target UGV. To determine the probability of detection, we first adjust the point source noise level by subtracting the background noise, estimated at 50 dB based on sound level meter readings from a military training area. Because sound decreases with the inverse square law with distance, we model spherical spread using the function $2log(\text{distance})$. After applying this function, we use the logistic function to convert the adjusted decibel level into a probability of detection. This ensures that louder noise levels correspond to higher detection probabilities, while quieter levels reduce the likelihood of detection.

2.2.2. Visual Detection

Visual detection accounts for both the line of sight and the total area that the UGV occupies in the seeker's vision. If the line of sight is obstructed, the visual detection probability is set to zero. Otherwise, the probability is determined based on the proportion of the UGV that remains visible. We utilize the proportion of the UGV visible within the seeker's field of view by analyzing how much of its shape remains unobstructed. Two key angles define visibility: the horizontal angle, which measures the seeker's lateral view of the UGV, and the vertical angle, which accounts for height and elevation differences. These angles determine how much of the UGV is visible. The trace calculation evaluates the intersection of the UGV's shape, found using the two described angles and some integration, with the seeker's field of view, modeled as a section of a sphere. The probability of detection is then based on the trace ratio, representing the visible portion of the UGV within the seeker's view. Similar to the audio detection model, we convert the visual coverage into a probability using a logistic function.

2.3. Energy Cost Mapping

The energy utilization of the ground vehicle is estimated using a one-degree-of-freedom (1DOF) equation of motion, modeling movement in the longitudinal direction. While more complex models (e.g., 3DOF or 6DOF) could improve accuracy, they introduce significant computational complexity, making 1DOF sufficient for this analysis. The total energy cost is determined by summing the forces acting on the vehicle's center of gravity, including, tractive force (required to achieve motion), brake force (resisting motion), drag force (air resistance), grade force (effect of terrain inclination), rolling resistance (friction between the wheels and surface). Velocity and acceleration profiles are calculated based on grid coordinates and terrain inclination, with motion restricted to cardinal and intermediate directions. From these profiles, tractive power, brake power, and regenerative power are estimated. The hybrid powertrain consists of a battery and a diesel generator. The net battery power is determined by subtracting the generator's contribution from the required tractive and regenerative power. A nonlinear battery model is used to simulate realistic energy storage behavior. Vehicle-specific parameters such as mass, drag coefficient, and rolling resistance are factored into these calculations to ensure accurate energy estimation.

3. Tactical Route Optimization for Mission Execution

Our methodology employs a Mixed Integer Nonlinear Programming (MINLP) approach to determine an optimal path through the terrain minimizing detection cost and ensuring energy feasibility. The network is represented as a directed graph with nodes and arcs, where each arc has an associated detection cost, travel time, and energy consumption. The model ensures that exactly one path is chosen from the start to the end node while maintaining the battery charge within allowable limits. All notation for the model can be found in Table 1.

Table 1: Notation for Optimization Model

Sets		
$\mathcal{N}$	Nodes in the network	
$\mathcal{N}^{\text{term}}$	Nodes in the network not including the start and end nodes	
$\mathcal{A}$	Arcs from node i to node j	
$\mathcal{A}_n^{\text{in}}$	Inflow arcs into node n	
$\mathcal{A}_n^{\text{out}}$	Outflow arcs from node n	
Parameters		**Units**
d_a	Detection metric along arc a	[unitless]
t_k	Travel time along arc a	[seconds]
e_k	Energy consumption along arc a	[joules]
$\hat{\mathrm{t}}$	Max travel time allowed	**seconds**
$\hat{\mathrm{b}}$	Max battery capacity	**joules**
a_k	The tail node for arc k	**unitless**

ISBN: 97819384969-9-8

Decision Variables		Units
Z_k^{s}	Binary variable representing if arc k is traversed	[binary]
X_k^{b}	Battery state of charge after traversing arc k	[kW]

$$\text{minimize} \quad \sum_{k \in \mathcal{K}} \text{d}_k Z_k^s \tag{3a}$$

The objective function, formulated as Equation (3a), minimizes the accumulated detection values along the selected path, where d_k represents the detection cost for each arc k. The decision variable Z_k^s, is a binary variable that indicates whether an arc k is selected in the optimal solution, thus contributing to the total cost if the path is chosen. By minimizing this cost, the solution aims to find the path that minimizes the total detection cost. Initial instances of our model aimed at a multiobjective optimization approach, balancing detection and energy usage; however, we choose to incorporate energy as a constraint.

$$\sum_{k \in \mathcal{A}_i^{\text{in}}} Z_k^{\text{s}} \leq 1 \quad \forall i \in \mathcal{N} \tag{4a}$$

$$\sum_{k \in \mathcal{A}_i^{\text{out}}} Z_k^{\text{s}} \leq 1 \quad \forall i \in \mathcal{N} \tag{4b}$$

$$\sum_{k \in \mathcal{A}_i^{\text{in}}} Z_k^{\text{s}} = \sum_{k \in \mathcal{A}_i^{\text{out}}} Z_k^{\text{s}} \quad \forall i \in \mathcal{N}^{\text{term}} \tag{4c}$$

Constraints (4a) and (4c) ensure that there is proper flow through the network. Constraints (4a) -(4b) ensure that the maximum number of arcs pointing into or out of a node is less than or equal to 1. This means that you can only go into a node once, but not all nodes are required to be visited. Constraint (4c) ensures that for every non-terminal node, the number of arcs into a node equals the number of arcs out of a node, which forces continuity of path and maintains the flow balance at each node.

$$\sum_{k \in \mathcal{A}_{start}^{\text{in}}} Z_k^{\text{s}} = 0 \tag{5a}$$

$$\sum_{k \in \mathcal{A}_{start}^{\text{out}}} Z_k^{\text{s}} = 1 \tag{5b}$$

$$\sum_{k \in \mathcal{A}_{end}^{\text{in}}} Z_k^{\text{s}} = 1 \tag{5c}$$

$$\sum_{k \in \mathcal{A}_{end}^{\text{out}}} Z_k^{\text{s}} = 0 \tag{5d}$$

Equations (5a)-(5d) are special considerations for the start and end nodes. Additionally, for terminal nodes, the number of arcs entering and exiting must be equal, while the start node has no incoming arcs but must have one outgoing arc, and the end node has one incoming arc but no outgoing arc. Together, these constraints guarantee that the flow is consistent throughout the network, with a clear start and end point.

$$0 \leq X_k^{\text{b}} \leq \hat{\text{b}} \quad \forall k \in \mathcal{A} \tag{6a}$$

$$X_k^{\text{b}} = \hat{\text{b}} Z_k^{\text{s}} \quad \forall k \in \mathcal{A}_{\text{start}}^{\text{out}} \tag{6b}$$

$$X_k^{\text{b}} = \left(\sum_{j \in \mathcal{A}_k^{\text{in}}} X_j^{\text{b}} - \text{e}_k \right) Z_k^{\text{s}}, \quad \forall k \in \mathcal{A},\ k \neq \text{start} \tag{6c}$$

ISBN: 97819384969-9-8

In order to integrate energy considerations into the model we implement constraints (6a)-(6c). These constraints connect the path selection variable Z_k^{s} with the energy storage system's state of charge variable X_k^{b}. Constraint (6a) enforces that the battery's state of charge at any point in the path remains within the appropriate bounds of the system. Constraint (6b) initializes the battery level at the start node, the battery is fully charged if the arc is selected going out of the start node. Finally, constraint (6c) models the battery depletion along the path, ensuring that the battery level at each arc is updated based on the energy consumption along the arc (if chosen) and the battery's accumulated state of charge for all of the incoming arcs. This guarantees that the energy feasibility of the selected path is maintained.

4. Results

We apply our methodology to a synthetic scenario using real-world data modeled by the terrain in the vicinity of Camp Buckner, which is located in a military training area. Figure 2a demonstrates a UGV path created by our model. The red circles and arrows depict the enemy's location and orientation. The size of the map is 1 km by 1 km. The node field is a two-layer, 12 by 12 grid with a total of 288 nodes and 2312 uni-directional arcs. The UGV starts its mission in the northwest of the map and ends at the southeast corner. The UGV begins in a non-charging state until it has moved beyond the second enemy's position. At this point along the path, the UGV has depleted the battery's state of charge and is required to recharge the battery by operating the generator before negotiating the higher terrain. To ensure the vehicle completes the mission, it maneuvers around the mountain to include a segment where it is oriented downhill to leverage the regenerative braking of the vehicle.

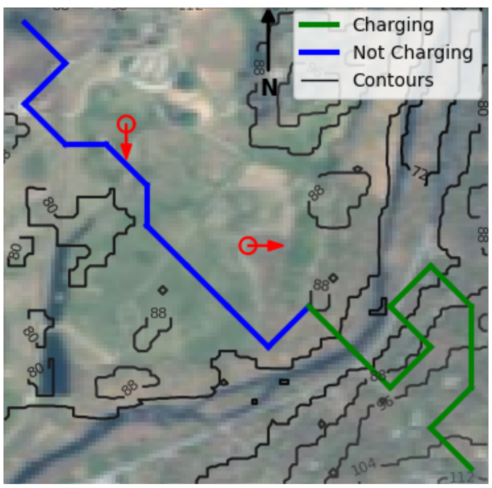

(a) Optimal path for minimizing detection while maintaining energy feasibility with two enemies in a 1x1 kilometer area

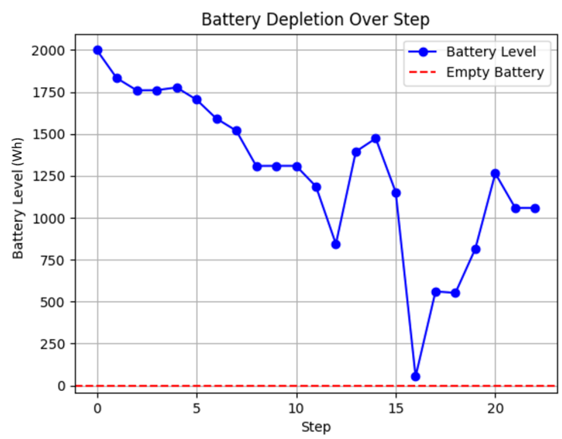

(b) On-board battery energy storage system's state of charge for the optimal path shown in Figure 2a

Figure 2: Results of the GhostRoute Modeling framework on terrain at the United States Military Academy's Training Area.

Figure 2b illustrates the battery's depletion throughout the UGV's traversal, highlighting the impact of elevation changes and generator activation on energy consumption. The battery was initialized at 2 kilowatt-hours. As the UGV progresses, its energy consumption increases due to terrain elevation changes, causing a steady decline in battery charge. Notably, the model prevents the UGV from charging when it is near enemy positions to lower detection costs. This constraint results in continuous battery depletion as the vehicle maneuvers through the environment. Once the battery reaches a critically low level, the generator is activated, ensuring the UGV has sufficient energy to continue its mission. The generator provides supplemental power as the UGV navigates up a steep incline.

For a commander, this modeling tool can provide different courses of action for a variety of mission types. For example, a mission may require follow on operations and therefore need the vehicle at a sufficient state of charge when it completes the path. This restriction is simply added as part of the inputs. The framework ensures that there exists a feasible path for the unmanned ground vehicle given the power constraint while utilizing the minimum level of detection. By integrating energy-aware path planning, commanders can ensure sustained operational capability and increased mission success rates for autonomous ground vehicles.

ISBN: 97819384969-9-8

5. Discussion

5.1. Limitations

Before fully implementing this system for UGVs, additional work is necessary to verify its accuracy and robustness. In particular, the visual and audio detection functions require further validation to ensure they effectively model real-world scenarios. Further testing should be conducted to confirm the probability of detection can be reliably used. This model also does not account for water. The satellite imagery does not currently provide a clear picture of where bodies of water are, thus it does not take them into account with our cost functions.

5.2. Future Work

A significant limitation of the current model is its lack of consideration for different types of terrain, for example water bodies, waterlogged terrain, or cliffs. To address this, improvements should be made to the satellite terrain assessment. Enhancing satellite-based assessments to distinguish between solid ground and impassable water bodies will ensure path viability. The implementation of LiDAR would also increase the accuracy of determining vegetation density. The model currently does not allow for charging in place. This is a significant disadvantage for military operations because it only models constant movement. If the model had the capability to charge in place it would allow for a further increase in mission capability for the UGV.

6. Conclusion

In this work, we have presented a methodology for autonomous vehicle route planning that balances energy efficiency and stealth to enhance mission success. By transforming open-source satellite data into geospatial detection fields through the evaluation of terrain, vegetation density, and enemy locations, our approach enables more informed decision-making in contested environments. Leveraging network structures and optimization techniques, we have demonstrated a strategy that minimizes energy consumption while simultaneously reducing the likelihood of detection. This dual-objective optimization ensures that unmanned ground vehicles can operate with greater survivability and endurance, crucial factors in military and high-risk applications. Our approach underscores the importance of integrating terrain-aware energy modeling with stealth optimization, addressing the inherent trade-offs between mission effectiveness and operational constraints. By considering these variables, the proposed algorithm ensures that UGVs can navigate more efficiently while maintaining a low-profile signature.

References

Almoaili, E., & Kurdi, H. (2020). Path Planning Algorithm for Unmanned Ground Vehicles (UGVs) in Known Static Environments. *Procedia Computer Science*, *177*, 57-63. doi: https://doi.org/10.1016/j.procs.2020.10.011

Blackmon, J. (2022). *Imporovements to visual and audio functions for optimized tactical route planning.* (Unpublished manuscript)

Huang, S., Tang, L., Hupy, J. P., Wang, Y., & Shao, G. (2021, Feb). A commentary review on the use of normalized difference vegetation index (ndvi) in the era of popular remote sensing. *Journal of Forestry Research*, *32*(1), 1–6. doi: 10.1007/s11676-020-01155-1

Jane, R., Parker, G. G., Weaver, W., Matthews, R., Rizzo, D., & Cook, M. (2017). Optimal Power Management of Vehicle Sourced Military Outposts. *SAE International Journal of Commercial Vehicles*, *10*(2017-01-0271), 132–143.

Juhari, K. A., Salleh, M. R., Muhamad, M. N., & Ito, T. (2013). 208 Navigation System for Unmanned Ground Vehicle. *The Proceedings of Manufacturing Systems Division Conference*, *2013*, 53-54. doi: 10.1299/jsmemsd.2013.53

Kendall, T. P., Killian, D. T., & Koch, M. J. (2023). Optimized tactical route planning. *Military Operations Research*, *28*(4), pp. 5–22. Retrieved 2025-04-11, from `https://www.jstor.org/stable/27274553`

Ma, Y., Hu, M., & Yan, X. (2018). Multi-Objective Path Planning for Unmanned Surface Vehicle with Currents Effects. *ISA Transactions*, *75*, 137-156. doi: https://doi.org/10.1016/j.isatra.2018.02.003

Macharet, D. G., Neto, A. A., & Shishika, D. (2021). Minimal Exposure Dubins Orienteering Problem. *IEEE Robotics and Automation Letters*, *6*(2), 2280-2287. doi: 10.1109/LRA.2021.3061004

Pfeiffer, B., Batta, R., Klamroth, K., & Nagi, R. (2007, 01). Path Planning for UAVs in the Presence of Threat Zones Using Probabilistic Modeling. *IEEE Transactions on Automatic Control*, *43*.

Rouse, J., Haas, R., Schell, J., & Deering, D. (1974). *Monitoring the vernal advancement and retrogradation (green wave effect) of natural vegetation* (Tech. Rep.). College Station, TX: Texas A&M University, Remote Sensing Center. (Final Report, NASA Goddard Space Flight Center, Greenbelt, MD)